Assessment of blood supply in superficial tissue by polarization-gated elastic light-scattering spectroscopy

Michael P. Siegel, Young L. Kim, Hemant K. Roy, Ramesh K. Wali, and Vadim Backman

We report the feasibility of monitoring both hemoglobin oxygen saturation and hemoglobin concentration in the superficial layer of tissue using polarization-gated elastic light-scattering spectroscopy. We detail our analysis technique, the experimental validation of our analysis, and the detection of an early increase in blood supply to the superficial layer of colon tissue in human patients with colonic adenomas as well as in an animal model of colon carcinogenesis. To the best of our knowledge, this study represents the first evidence that polarization gating can be used as a spectroscopic tool to quantify hemoglobin concentration as well as oxygen saturation in the uppermost tissue layer.

OCIS codes: 170.1470, 170.4580, 170.6510, 290.1350.

1. Introduction

Knowledge of hemoglobin oxygen saturation (S_{O_2}) and total hemoglobin concentration (C_{Hb}) in tissue is useful for many medical applications. In a diagnostic capacity, cancer-induced angiogenesis or vasodilation would manifest as an increased local hemoglobin concentration. Additionally, hypoxia is known to be a distinctive feature of many malignancies, which can be detected as a reduction in S_{O_2}.[1] S_{O_2} is also known to be a useful marker for assessing the potential effectiveness or monitoring the progress of certain cancer treatments.[2–4] Last, there is significant interest in the monitoring of C_{Hb} and S_{O_2} to assess functional properties of tissues such as the brain.[5]

Optical techniques, because of their noninvasive nature and the distinct absorption spectrum of hemoglobin, are some of the most popular methods used to quantify S_{O_2} and C_{Hb} in human tissue. Near-infrared (NIR) spectroscopy techniques are often used to measure these quantities because of the relative ease with which NIR light can penetrate tissue.[2,6–8] Diffusion theory is another reliable basis for the determination of the optical properties of tissue.[9–12] Diffusion theory was used by Mourant *et al.*, for example, to determine absorption coefficients of tissue phantoms.[13] This work was then extended to measure internal concentrations of drugs with unique absorption bands *in vivo*.[14] Diffuse reflectance spectroscopy is another popular technique used to assess the properties of internal absorbers such as hemoglobin within a tissue.[15–17] These techniques typically provide information regarding relatively large tissue depths. Franceschini *et al.* showed that, for two-layer turbid media, diffusion analysis in the NIR range provides information regarding the bottom layer alone when the top-layer thickness is less than 0.4 cm.[18]

Less attention has been paid to the quantification of hemoglobin properties in the superficial tissue layer. That is not to say, however, that work in this arena has never been done. Amelink *et al.*, for example, developed their novel differential path-length spectroscopy technique to study near-surface tissues and were able to accurately measure optical properties of superficial tissue.[19,20] This group even extended their technique to the measurement of S_{O_2} and C_{Hb}. In colon tissue the superficial layer is the mucosa, which contains the epithelium as well as subepithelial connective tissue, microvasculature, and smooth muscle cells. The epithelium is known to be the origin of more than 85% of all human cancers,[21] making accurate assessment of this superficial layer vital to the early detection of cancer.

In this paper we report on the use of polarization-gated elastic light-scattering spectroscopy to measure S_{O_2} and C_{Hb} in the superficial layer of tissue, using basic spectral analysis. Polarization gating is a

M. P. Siegel (cgul72@hotmail.com), Y. L. Kim, and V. Backman are with the Department of Biomedical Engineering, E310, Northwestern University, 2145 Sheridan Road, Evanston, Illinois 60208. H. K. Roy and R. K. Wali are with the Department of Internal Medicine, Evanston-Northwestern Healthcare, Evanston, Illinois 60201.

Received 12 April 2005; revised 19 August 2005; accepted 25 August 2005.

0003-6935/06/020335-08$15.00/0

method used with optical spectroscopy techniques that subtracts out the contribution from diffuse photons depolarized by multiple scattering events. Since photons that penetrate more deeply into a tissue are more likely to undergo multiple scattering events, polarization gating effectively selects photons that have been scattered from very shallow tissue depths. This depth selectivity has been shown to be limited to depths equal to a few mean free paths, therefore making it a widely respected method for the probing of superficial tissue structures within approximately 50 μm of the surface.[22]

A significant body of research exists that utilizes polarization gating as a reliable means for selecting photons scattered from shallow tissue depths.[21–25] Myakov *et al.* integrated polarized reflectance spectroscopy with a fiber-optic probe and showed that it could be reliably used to reduce the influence of deeply penetrating photons.[26] A number of researchers, including Jacques *et al.*, have used polarization gating techniques to clearly image near-surface structures.[23] Since deeply penetrating photons that make up the diffuse component removed by polarization gating are more likely to encounter hemoglobin in deeply set blood vessels, polarization gating is a simple way to reduce characteristic hemoglobin absorption bands. We show that the contribution from hemoglobin absorption that remains after polarization gating can be used to quantify hemoglobin residing in near-surface microvasculature.

After validating our technique, we applied it to both an animal model of carcinogenesis, azoxymethane-(AOM-) treated rats, and a human study in which we looked for the presence of an early increase in blood supply (EIBS) to the superficial mucosa. EIBS is a novel marker for the detection of early carcinogenesis,[27] characterized by an increase in blood supply to the superficial mucosa before the appearance of dysplastic lesions. Therefore the ability to measure S_{O_2} and C_{Hb} in the superficial tissue layer is uniquely suited for the detection of this diagnostic marker.

2. Materials and Methods

A. Experimental Setup

A schematic diagram of our setup is shown in Fig. 1. A collimated beam from a 75 W xenon arc lamp (Oriel) was passed through one dichroic sheet polarizer (Melles-Griot) and then a beam splitter (Newport). The beam then contacted our sample, and light backscattered from this sample traveled back through the beam splitter to be collected by a lens (Melles-Griot). This beam splitter was oriented at an angle of approximately 15° to the normal to reduce specular reflection. A second polarizer was positioned between this lens and our collection system, which consisted of a spectrograph (Acton Research Corp.) coupled to a CCD camera (Roper Scientific Inc.). By adjusting the second polarizer we independently collected light polarized parallel to the incident beam (copolarized, $I_{\parallel}$) and light polarized perpendicular to the incident beam (cross-polarized, $I_{\perp}$) over a spectral range from $\lambda = 500$ to 600 nm. The polarization-gated signal was taken as the difference between copolarized and cross-polarized signals. This difference was normalized against the sum of the copolarized and cross-polarized spectra from a polytetrafluoroethylene reflectance standard (Ocean Optics).

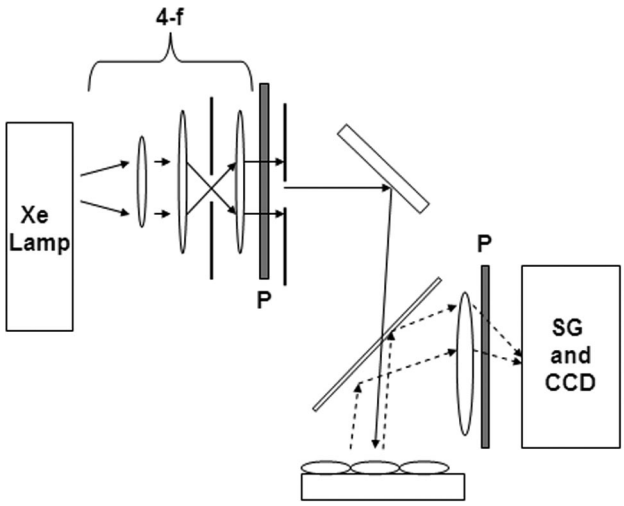

Fig. 1. Schematic diagram of our system. The light from a xenon lamp is collimated using a 4-*f* system and then passed through the first polarizer P. It is then directed onto the sample, and backscattered light passes through another polarizer before reaching a spectrograph (SG) coupled to a CCD camera.

$$\Delta I(\lambda) = \frac{I_{\parallel}(\lambda) - I_{\perp}(\lambda)}{I_{\parallel}^{RS}(\lambda) + I_{\perp}^{RS}(\lambda)}, \tag{1}$$

where $\Delta I(\lambda)$ is the polarization-gated signal, and $I^{RS}(\lambda)$ represents the signal taken from the reflectance standard. Sample spectra taken from a suspension of polystyrene microspheres in hemoglobin and water are shown in Fig. 2.

B. Data Analysis

To extract values for S_{O_2} and C_{Hb} from our signal, we developed an algorithm using MATLAB (MathWorks). It is known that Beer's law cannot be directly applied to the analysis of scattered light because of unknown path length and unknown attenuation due to scattering.[14,28] However, Beer's law served as the inspiration for our analysis technique as we assumed attenuation due to absorption to have an inverse exponential relationship with absorber concentration. This assumption can be expressed as follows:

$$\Delta I(\lambda) = \Delta I_{scattering}(\lambda)\exp[-\alpha A_{PG}(\lambda)], \tag{2}$$

where $\Delta I_{scattering}(\lambda)$ represents the polarization-gated spectrum that would be obtained from a sample if it were devoid of any absorber; $A_{PG}(\lambda)$ represents the polarization-gated spectrum of all absorbers that actually are present; and α is a nominal coefficient, which would be the product of path length and con-

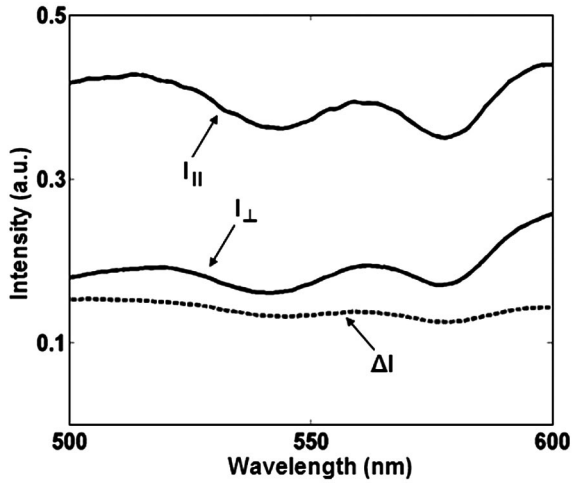

Fig. 2. Spectra taken from a sample consisting of 4.3 μm polystyrene beads suspended in a solution of water and hemoglobin. Note the characteristic oxygenated hemoglobin absorption bands in all three spectra at approximately 542 and 576 nm. $I_{\parallel}$ and $I_{\perp}$ were normalized against the copolarized and cross-polarized spectra from our reflectance standard, and ΔI was normalized against the sum of the copolarized and cross-polarized reflectance spectra.

centration under the constraints of Beer's law. We hypothesized that α would serve as a reliable indicator of absorber concentration over a wide range of tissue properties and sought to experimentally validate this hypothesis.

First, the spectrum of oxygenated hemoglobin (HbO_2) needed to be distinguished from that of deoxygenated hemoglobin (Hb). In this case, $A_{PG}(\lambda) = A_{PG}{}^{HbO_2}(\lambda) + A_{PG}{}^{Hb}(\lambda)$, where $A_{PG}{}^{HbO_2}(\lambda)$ and $A_{PG}{}^{Hb}(\lambda)$ are the spectra of HbO_2 and Hb, respectively. This case also required independent coefficients, α_{Hb} and α_{HbO_2}, to account for the different contributions of Hb and HbO_2, respectively. To obtain the individual spectra for HbO_2 and Hb, we measured a solution of 1 g/l HbO_2 in water using our system. This accounted for deviations from published spectra caused by any error in the calibration of our system. The solution was placed in a glass-bottomed culture slide directly on top of the reflectance standard and measured to obtain a spectrum for HbO_2. It was then deoxygenated by adding sodium dithionite to a final concentration of 10 g/l to measure the spectrum for Hb.

The remaining unknown for our analysis was prior knowledge of $\Delta I_{scattering}(\lambda)$. Such knowledge would allow us to find α_{Hb} and α_{HbO_2} responsible for the best-fit approximation to the expected $\Delta I_{scattering}(\lambda)$. To fill this gap we assumed $\Delta I_{scattering}(\lambda)$ to have a smooth linear decline between $\lambda = 500$ and 600 nm and to lack spectral features of hemoglobin absorption, which include absorption bands at 542 and 576 nm in the case of HbO_2 and 555 nm in the case of Hb. It is generally known that light with longer wavelength scatters less and thus penetrates more deeply into a scattering medium. This principle is manifested as a decrease in intensity over wavelength. Over our narrow spectral region, this assumption turned out to be highly reasonable. Thus our algorithm tested all values of α_{Hb} and α_{HbO_2} over a chosen range and found those responsible for the best linear approximation of $\Delta I_{scattering}(\lambda)$ in the least-squares sense. With these values in hand, S_{O_2} and C_{Hb} could be found using the following simple relationships:

$$S_{O_2} = \frac{\alpha_{HbO_2}}{\alpha_{HbO_2} + \alpha_{Hb}} \times 100\,\%, \tag{3}$$

$$C_{Hb} \propto \alpha = \alpha_{Hb} + \alpha_{HbO_2}. \tag{4}$$

The validity of Eqs. (3) and (4) was verified using the tissue phantom experiments outlined below.

C. Tissue Phantom Model

To validate the accuracy of our analysis technique, we performed a series of tissue phantom studies using polystyrene microspheres (Duke Scientific) suspended in de-ionized water. Microspheres with a diameter of 4.3 or 4.5 μm and a standard deviation of 25% were used in all cases. Concentrations were carefully controlled to maintain specific scattering properties throughout all experiments. All values for the scattering coefficient μ_s were calculated at $\lambda = 550$ nm using Mie theory.[29]

S_{O_2} calculations were validated using the method reported by Hull and Foster in 1997.[2] We rinsed 80 μl of fresh, whole human blood from one healthy volunteer with 1× phosphate buffered saline (PBS), pH 7.4, and centrifuged to separate out the red blood cells. These cells were then resuspended in 1 ml of PBS to a volume fraction of 3.2%, assuming a 40% hematocrit. A small quantity of this solution was added to a polystyrene bead suspension with $\mu_s = 73.3\ cm^{-1}$ and deoxygenated by the addition of a small amount of dry baker's yeast. The gradual deoxygenation of this suspension was monitored using an oxygen-sensitive microelectrode (Microelectrodes, Inc.). The final volume fraction of red blood cells was 0.64%. This procedure was then repeated using lyophilized human hemoglobin (Sigma-Aldrich) to a concentration of 1 g/l instead of red blood cells. In this case, $\mu_s = 96.0\ cm^{-1}$.

As a standard for comparison, we used the subroutine reported by Kelman[30] to compute the hemoglobin saturation at oxygen partial pressures ranging from 0 to 120 mm Hg at $T = 20$ °C and pH 7.4. By using this method, we were able to compare our results with those expected for our precise experimental conditions. Values for Hill's coefficient and the partial pressure of oxygen at which hemoglobin is 50% saturated (P_{50}) were used for quantifiable comparison.

The usefulness of our factor α as a measure of C_{Hb} was validated by preparing three 5 ml suspensions with $\mu_s = 38.4$, 115, and 223 cm^{-1}, respectively. Suspensions were held in a 58 mm glass Petri dish and had a geometric thickness of 1.9 mm. Concurrently, we prepared suspensions with the same scattering properties but also containing lyophilized human hemoglobin to concentrations of 19.0, 17.0, and 14.2 g/l,

respectively. These second suspensions were gradually incorporated into the first to vary their true C_{Hb} without changing their scattering properties.

To verify the relevance of the above tissue phantom studies with respect to *in vivo* tissue architecture (i.e., a thin, scattering epithelial layer lacking absorbers above a thick layer containing both scatterers and absorbers), we performed a series of two-layer phantom studies. In these studies, the bottom layer was an agarose gel (2 g agarose and 100 ml de-ionized water) containing polystyrene microspheres and hemoglobin with geometric thickness of 3.8 mm. The concentration of microspheres was held constant to keep $\mu_s = 115\ \text{cm}^{-1}$ through all trials while the concentration of hemoglobin was varied between 0.34 and 0.80 g/l . The top layer consisted of an aqueous suspension of polystyrene microspheres with $\mu_s = 115\ \text{cm}^{-1}$ and geometric thickness of 87 μm for our first trial and $\mu_s = 38.4\ \text{cm}^{-1}$ and geometric thickness of 260 μm for our second trial. No hemoglobin was present in the top layer. The top layer simulated an avascular thin layer of epithelium, and the second layer mimicked subepithelial connective tissue, microvasculature, and smooth muscle immediately beneath the epithelium. If results of this two-layer study are in agreement with those from the one-layer study, then its relevance will have been validated.

D. Animal Studies

The institutional animal care and use committee of Evanston-Northwestern Healthcare approved all studies reported in this paper. Four male Fisher 344 rats were randomly placed into two groups of two—the test group, which received two injections of AOM (15 mg/kg) per week and the control group, which received two injections of saline per week. AOM is a trusted colon carcinogen in rats; rats treated with AOM develop the earliest known marker of colon carcinogenesis, aberrant crypt foci (ACF), after approximately 5 weeks.[27] Approximately 20 weeks after the second carcinogen injection, adenomas start appearing with frank adenocarcinomas requiring 35–40 weeks to develop.[21] Only 2 weeks after AOM treatment (prior to occurrence of ACF), rats were euthanized by CO_2 and their colons were removed and separated into proximal and distal segments. These segments were preserved in PBS and measured using our instrument within 2 h of sacrifice. In our analysis, we looked at only distal colon segments because the distal colon is known to reliably develop cancerous adenomas after AOM treatment, whereas the proximal colon is not.[27]

E. Human Studies

Biopsies were taken with fully informed consent from the cecum of 100 patients undergoing routine colonoscopy. Patients whose present or previous colonoscopies revealed no sign of neoplasia (adenoma or carcinoma) were placed in the control group. Patients with cecal adenomas were placed in the test group. In the case of an adenoma, biopsies were taken of tissue approximately 2 cm away from the adenoma and not of the adenoma directly. All samples were preserved in PBS, placed on a glass slide, and measured using our system within 2 h of surgery.

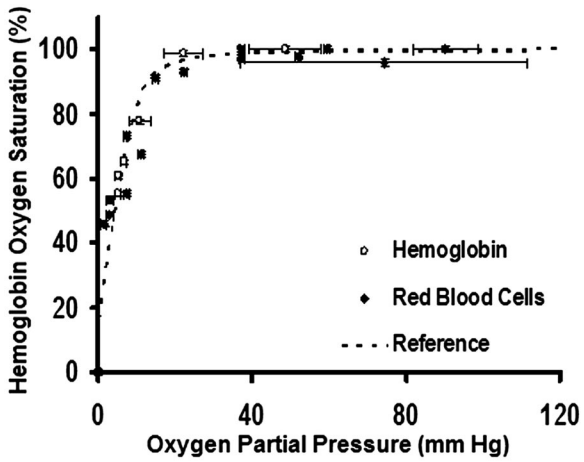

Fig. 3. Recreation of the hemoglobin oxygen dissociation curve using the spectral analysis of a polarization-gated signal. The dashed curve represents the curve as predicted by Kelman's subroutine.

3. Results

A. Phantom Model

Using the same procedure reported by Hull and Foster,[2] we validated our S_{O_2} measurements using a best-fit approximation of Hill's equation to our data with a least-squares approach. First we found values for Hill's coefficient and P_{50} using data gathered in our yeast phantom experiments. These values were then compared with Hill's coefficient and P_{50} obtained using the same least-squares approach to the hemoglobin dissociation curve found by the subroutine reported by Kelman.[30] This predicted value for Hill's coefficient was 1.84 with $P_{50} = 4.07$ mm Hg. Calculated Hill's coefficients from our phantom experiments were 1.77 ± 0.15 and 1.67 ± 0.11 for the red blood cells and the lyophilized hemoglobin, respectively. P_{50}'s were 5.57 mm Hg $\pm$ 0.72 and 4.42 mm Hg $\pm$ 0.53, respectively. Within the bounds of experimental error, these values were in excellent agreement with those that we predicted (Fig. 3).

To determine the accuracy of these calculations we found S_{O_2} of polystyrene bead phantoms with known 100% HbO_2 over a wide range of concentrations. The results showed a high level of accuracy with $S_{O_2} = 98.5\% \pm 0.8\%$.

The results showed that α had a strong linear correlation with C_{Hb} (Fig. 4) over our range of physiological hemoglobin concentrations and scattering coefficients. We used the results of this experiment to find the scaling factor by which α can be converted to an absolute hemoglobin concentration in grams per liter. This factor was found as the average slope of α versus C_{Hb} for all μ_s, and its value was 0.876. We also

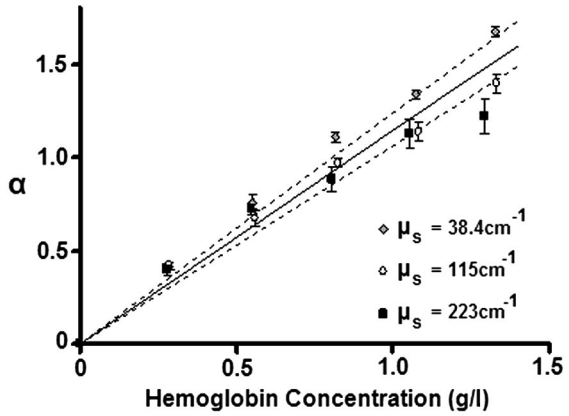

Fig. 4. Relative concentration of hemoglobin α calculated over a range of physiological values. The solid line represents the curve used to calibrate α for calculations of absolute hemoglobin concentration. Dashed lines represent linear approximations for μ_s = 38.4 and 223 cm^{-1}. We used these curves to identify a maximum reasonable deviation in calculations of hemoglobin concentration due to scattering.

determined the error in this calibration as the maximum deviation from this factor detected in our phantom study. Specifically, error was calculated as the differences between our calibration curve and the linear approximations of α versus C_{Hb} for μ_s = 38.4 and 223 cm^{-1}. After the calibration was performed, it was possible to measure absolute hemoglobin concentration, with a known level of error, over a wide range of scattering properties even when μ_s is unknown. As discussed below (Subsection 3.B), this procedure can clearly rule out unknown scattering properties as a source of error in hemoglobin concentration calculations. To test the accuracy of our optical measurement of blood content in superficial tissue in the presence of a thin avascular epithelial layer, we conducted studies with the two-layer physical tissue models. In these models, the optical properties of each layer were chosen to mimic those of real colonic tissue. As shown in Fig. 5, we demonstrated that the

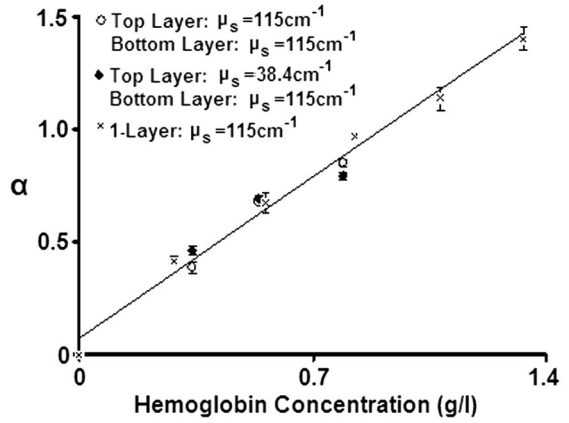

Fig. 5. Results of two-layer phantom study. The agreement between these data and those gathered during the single-layer phantom study demonstrates the relevance of our technique for *in vivo* applications.

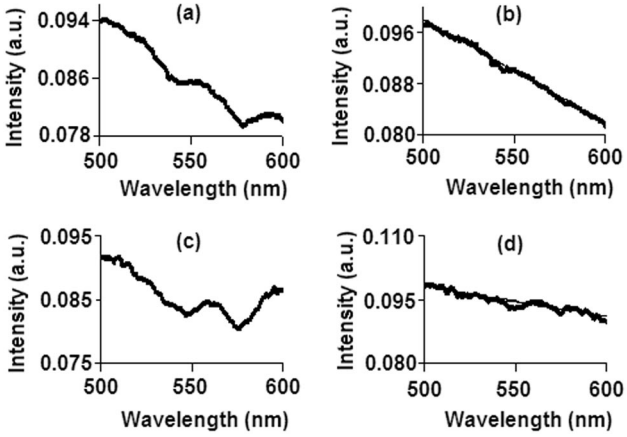

Fig. 6. Spectra taken from human biopsy samples. (a) Polarization-gated spectrum taken from a control group patient prior to hemoglobin removal. (b) Polarization-gated spectrum from (a) after hemoglobin removal. (c) Polarization-gated spectrum taken from a test group patient prior to hemoglobin removal. (d) Polarization-gated spectrum from (d) after hemoglobin removal. In both (b) and (d), the dashed curves represent the linear approximation of the spectrum.

presence of a thin, scattering top layer has no effect on results generated by our algorithm and that our one-layer phantom study is therefore reliable.

B. Animal and Human Studies

Sample spectra taken from human data are depicted in Fig. 6. Spectra obtained from the rat study are similar in appearance. We detected a statistically significant increase in the blood supply to the superficial mucosa of the colon in AOM-treated rats as early as 2 weeks after initiation of carcinogenesis as well as in human patients with one or more adenomas (Fig. 7). Positive error bars in Fig. 7 represent calculated C_{Hb} if μ_s = 38.4 cm^{-1}, and negative error bars represent calculated C_{Hb} if μ_s = 223 cm^{-1}. It is clear in both

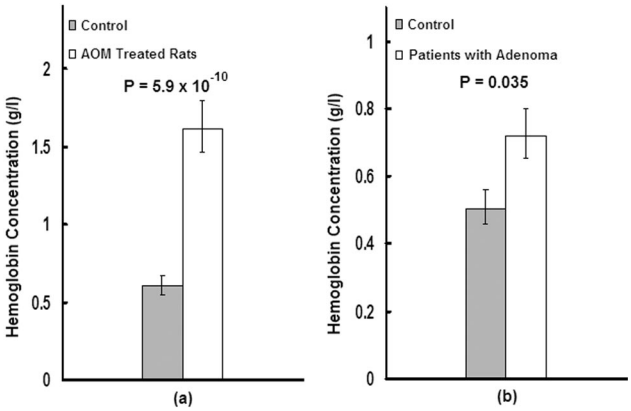

Fig. 7. Display of EIBS in both (a) the AOM rat model and (b) the human colon biopsies. To obtain these results we used the calibration curve in Fig. 4 to convert α to true C_{Hb}. This relation was C_{Hb} = 0.876α. Error bars represent possible deviation on account of scattering ranging from μ_s = 38.4 to 223 cm^{-1}. Final population sizes were 4 rats and 24 human patients.

models that a change in scattering properties within this range is not responsible for a false diagnosis of EIBS.

No significant difference in S_{O_2} was detected in either case. The average S_{O_2} for human control patients was 75.9% ± 12.3%, and for patients with adenomas the average S_{O_2} was 79.4% ± 5.7%. S_{O_2} in the superficial mucosa of AOM-treated rats was approximately 0% for all samples. This discrepancy may seem interesting at first glance, but actually met with our prior expectations. The reasons behind this are discussed in Section 4.

4. Discussion

We have demonstrated the ability to use polarization-gated elastic light-scattering spectroscopy to accurately measure the oxygen saturation of hemoglobin (S_{O_2}) and hemoglobin concentration (C_{Hb}) in the superficial tissue layer. Furthermore, this capability was extended to the detection of an EIBS in humans with cecal adenomas as well as AOM-treated rats after 2 weeks of initiation. The accuracy of our measurements was successfully validated using polystyrene bead phantoms.

To the best of our knowledge, this work represents the first evidence that polarization gating can be used to assess blood supply and hemoglobin oxygen saturation in shallow tissue depths. Polarization gating is often used with spectroscopic or imaging techniques to remove the contribution of hemoglobin to a signal by removing the background created by deeply penetrating photons. However, as is evident in Figs. 2 and 6, the entire contribution by hemoglobin absorption is not always removed by simple polarization gating. The remaining contribution is likely a result of subepithelial blood vessels that lie within 50 μm of the surface[27] in the case of colon tissue. Until now, accurate, noninvasive assessment of this blood has not been possible.

Our method is based on a relatively simple shape-fitting procedure over a spectrum spanning 100 nm, making it very fast and accurate. Measurements of S_{O_2} required no calibration and had less than 1% error. Measurements of C_{Hb} had an average standard error of less than 5% for constant μ_s. R^2 values for $\mu_s = 38$, 115, and 223 cm^{-1} were 0.996, 0.989, and 0.969, respectively, showing a strong linear correlation between our factor α and actual C_{Hb} in all cases. On the basis of these strong linear relationships, we were able to carry out a straightforward calibration and extend our technique to the measurement of absolute hemoglobin concentration.

One possibility would be to assume that hemoglobin concentrations in our animal and human studies were equal between test and control groups, and that the change we observed was due to a difference in scattering alone. For example, a drastic decrease in μ_s would allow photons to penetrate more deeply into tissue before being depolarized, thus increasing their likelihood of being absorbed by hemoglobin, even if overall hemoglobin concentration remained constant. In simple terms, low μ_s would be falsely represented as high C_{Hb}. To address this concern, the increases in C_{Hb} seen in both our rat study and our human study would require a change in scattering that is out of the realm of normal variation in tissue properties, even in the case of malignant tissue.[31–33] Not only would the change in scattering have needed to exceed the sixfold difference in μ_s accounted for by our experimental calibration, but the scattering coefficient of precancerous tissue would need to be far less than that of normal tissue. According to the literature, this is seldom the case. Collier *et al.* reported μ_s of normal cervical tissue to be 22 cm^{-1}, whereas precancerous cervix had $\mu_s = 69$ cm^{-1}, marking nearly a threefold increase.[32] Furthermore, Beek *et al.* reported μ_s for colon adenocarcinomas in rats to be 280 ± 20 cm^{-1} at $\lambda = 632.8$ nm, indicating that μ_s of the precancerous tissue used in both of our studies was more likely near the upper limit of our calibration range than the lower limit.[34] We therefore concluded that our technique is a reliable means of comparing hemoglobin properties as long as the comparison is being made between similar tissue types.

EIBS is a novel biomarker, whose origin has not yet been established. Our current hypothesis focuses on the potential early overexpression of inducible nitrous oxide synthase. This would lead to an increase in vasodilation and an increased supply of blood without angiogenesis. It is important to distinguish EIBS from the well-known increase in blood supply resulting from angiogenesis, which is necessary to provide nutrients to adenomas or tumors with a diameter of more than ~1 mm.[4] To illustrate this point, human biopsies were taken approximately 2 cm away from adenomas and rat colons were examined after only 2 weeks of AOM treatment. Typically, angiogenesis associated with colon carcinogenesis does not occur until approximately 40 weeks after the administration of AOM.[21] Therefore human measurements were not taken from locations likely to contain new blood vessels and rat measurements were taken at a time point known to predate the conception of angiogenesis.

Neither our animal study nor our human study revealed a significant difference in hemoglobin oxygen saturation between test and control groups. Human tissue had reasonable S_{O_2} values, in the vicinity of 75% saturation. If it is true that subepithelial capillaries account for blood measured by our system, a value somewhere between approximately 100% saturated blood found in arteries and approximately 50% saturated blood found in veins is expected. The near 0% S_{O_2} values in the superficial layer of rat colon, on the other hand, was an interesting finding. In terms of explanation, rats were euthanized using CO_2, meaning that they were deprived of oxygen prior to death. Low S_{O_2} was, in fact, the reason for their deaths and this was evident in our measurements. Therefore our animal study and our human study both met prior expectations for S_{O_2}, which helped to further validate our technique.

Final consideration must be paid to any variations in these results on account of the distribution of hemoglobin within human tissue. Evidence exists that both the packaging of hemoglobin into red blood cells[35] and the inhomogeneous distribution of blood within biological tissue[36] have an effect on the absorption spectrum of hemoglobin. The spectrum we used in our analysis proved to be reliable for studies on phantoms containing either red blood cells or stripped hemoglobin. Additionally, values for S_{O_2} and C_{Hb} that we detected in the human biopsies were well within a reasonable physiological range. We therefore conclude that any error resulting from such affects is negligible in this case.

In summary, we have described a reliable approach to quantify hemoglobin oxygen saturation and hemoglobin concentration in superficial tissue using polarization-gated elastic light-scattering spectroscopy and a basic spectral analysis. We detected an early increase in blood supply to the subepithelial portion of the mucosa and submucosa in human colon biopsies of patients with adenomas as well as rat colons after 2 weeks of treatment with AOM. This study lays the foundation for future *in vivo* studies using fiber-optic technology.

This study was supported by National Institutes of Health grant R01CA109861. Y. L. Kim is supported in part by the Cancer Research and Prevention Foundation.

References

1. P. Vaupel, O. Thews, and M. Hoeckel, "Treatment resistance of solid tumors: role of hypoxia and anemia," Med. Oncol. **18,** 243–259 (2001).
2. E. L. Hull and T. H. Foster, "Noninvasive near-infrared hemoglobin spectroscopy for *in vivo* monitoring of tumor-oxygenation and response to oxygen modifiers," in Proc. SPIE **2979,** 355–364 (1997).
3. H. W. Wang, M. E. Putt, M. J. Emanuele, D. B. Shin, E. Glatstein, A. G. Yodh, and T. M. Busch, "Treatment-induced changes in tumor oxygenation predict photodynamic therapy outcome," Cancer Res. **64,** 7553–7651 (2004).
4. P. Vaupel and L. Harrison, "Tumor hypoxia: causative factors, compensatory mechanisms, and cellular response," Oncologist **9,** (Suppl. 5) 4–9 (2004).
5. A. K. Dunn, A. Devor, H. Bolay, M. L. Andermann, M. A. Moskowitz, A. M. Dale, and D. A. Boas, "Simultaneous imaging of total cerebral hemoglobin concentration, oxygenation, and blood flow during functional activation," Opt. Lett. **28,** 28–30 (2003).
6. H. Liu, D. A. Boas, Y. Zhang, A. G. Yodh, and B. Chance, "Determination of optical properties of blood oxygenation in tissue using continuous NIR light," Phys. Med. Biol. **40,** 1983–1993 (1995).
7. S. Srinivasan, B. W. Pogue, S. Jiang, H. Dehghani, C. Kogel, S. Soho, J. J. Gibson, T. D. Tosteson, S. P. Poplac, and K. D. Paulsen, "Interpreting hemoglobin and water concentration, oxygen saturation, and scattering measured in vivo by near-infrared breast tomography," Proc. Natl. Acad. Sci. USA **100,** 12349–12354 (2003).
8. S. J. Matcher and C. E. Cooper, "Absolute quantification of deoxyhaemoglobin concentration in tissue near infrared spectroscopy," Phys. Med. Biol. **39,** 1295–1312 (1994).
9. T. J. Farrell and M. S. Patterson, "A diffusion theory model of spatially resolved, steady-state diffuse reflectance for the noninvasive determination of tissue optical properties *in vivo*," Med. Phys. **19,** 879–888 (1992).
10. V. Venugopalan, J. S. You, and B. J. Tromberg, "Radiative transport in the diffusion approximation: an extension for highly absorbing media and small source-detector separations," Phys. Rev. E **58,** 2395–2407 (1998).
11. S. Fantini, M. A. Franceschini, and E. Gratton, "Semi-infinite-geometry boundary problem for the light migration in highly scattering media: a frequency-domain study in the diffusion approximation," J. Opt. Soc. Am. B **11,** 2128–2138 (1994).
12. A. Kienle, L. Lilge, M. S. Patterson, R. Hibst, R. Steiner, and B. C. Wilson, "Spatially resolved absolute diffuse reflectance measurements for noninvasive determination of the optical scattering and absorption coefficients of biological tissue," Appl. Opt. **35,** 2304–2314 (1996).
13. J. R. Mourant, T. Fuselier, J. Boyer, T. M. Johnson, and I. J. Bigio, "Predictions and measurements of scattering and absorption over broad wavelength ranges in tissue phantoms," Appl. Opt. **36,** 949–957 (1997).
14. J. R. Mourant, T. M. Johnson, G. Los, and I. J. Bigio, "Noninvasive measurements of chemotherapy drug concentrations in tissue: preliminary demonstrations of *in vivo* measurements," Phys. Med. Biol. **44,** 1397–1417 (1999).
15. W. T. Knoefel, N. Kollias, D. W. Rattner, N. S. Nishioka, and A. L. Warshaw, "Reflectance spectroscopy of pancreatic microcirculation," J. Appl. Physiol. **80,** 116–123 (1996).
16. G. Zonios, L. T. Perelman, V. Backman, R. Manoharan, M. Fitzmaurice, J. Van Dam, and M. S. Feld, "Diffuse reflectance spectroscopy of human adenomatous colon polyps *in vivo*," Appl. Opt. **38,** 6628–6637 (1999).
17. A. A. Strantonnikov and V. B. Loschenov, "Evaluation of blood oxygenation *in vivo* from diffuse reflectance spectra," J. Biomed. Opt. **6,** 457–467 (2001).
18. M. A. Franceschini, S. Fantini, L. A. Paunescu, J. S. Maier, and E. Gratton, "Influence of a superficial layer in the quantitative spectroscopic study of strongly scattering media," Appl. Opt. **37,** 7447–7458 (1998).
19. A. Amelink and H. J. C. M. Sterenborg, "Measurement of the local optical properties of turbid media by differential path-length spectroscopy," Appl. Opt. **43,** 3048–3054 (2004).
20. A. Amelink, H. J. C. M. Sterenborg, M. P. L. Bard, and S. A. Burgers, "*In vivo* measurement of the local optical properties of tissue by use of differential path-length spectroscopy," Opt. Lett. **29,** 1087–1089 (2004).
21. Y. L. Kim, Y. Liu, R. K. Wali, H. K. Roy, M. J. Goldberg, A. K. Kromin, K. Chen, and V. Backman, "Simultaneous measurement of angular and spectral properties of light scattering for characterization of tissue microarchitecture and its alterations in early precancer," IEEE J. Sel. Top. Quantum Electron. **9,** 243–255 (2003).
22. Y. Liu, Y. L. Kim, X. Li, and V. Backman, "Investigation of depth selectivity of polarization gating for tissue characterization," Opt. Express **13,** 601–611 (2005).
23. S. L. Jacques, J. C. Ramella-Roman, and K. Lee, "Imaging skin pathology with polarized light," J. Biomed. Opt. **7,** 329–340 (2002).
24. J. M. Schmitt, A. H. Gandjbakhche, and R. F. Bonner, "Use of polarized light to discriminate short-path photons in a multiply scattering medium," Appl. Opt. **31,** 6535–6546 (1992).
25. V. Backman, R. Gurjar, K. Badizadegan, L. Itzkan, R. R. Dasari, L. T. Perelman, and M. S. Feld, "Polarized light scattering spectroscopy for quantitative measurement of epithelial cellular structures in situ," IEEE J. Sel. Top. Quantum Electron. **5,** 1019–1026 (1999).
26. A. Myakov, L. Nieman, L. Wicky, U. Utzinger, R. Richards-

Kortum, and K. Sokolov, "Fiber optic probe for polarized reflectance spectroscopy *in vivo*: design and performance," J. Biomed. Opt. **7,** 388–397 (2002).
27. R. K. Wali, H. K. Roy, Y. L. Kim, Y. Liu, J. L. Koestier, D. P. Kunte, M. J. Goldberg, V. Turzhitsky, and V. Backman, "Increased microvascular blood content is an early event in colon carcinogenesis," Gut **54,** 654–660 (2005).
28. V. P. Dick, "Applicability of Beer's law for dispersion media with a high concentration of particles," Appl. Opt. **37,** 4998–5004 (1998).
29. H. C. van de Hulst, *Light Scattering by Small Particles* (Dover, 1995).
30. G. R. Kelman, "Digital computer subroutine for the conversion of oxygen tension into saturation," J. Appl. Physiol. **21,** 1375–1376 (1966).
31. R. Marchesini, A. Bertoni, S. Andreola, E. Melloni, and A. E. Sichirollo, "Extinction and absorption coefficients and scattering phase functions of human tissues *in vitro*," Appl. Opt. **28,** 2318–2324 (1989).
32. T. Collier, A. Dizem, A. Malpica, M. Follen, and R. Richards-Kortum, "Determination of epithelial tissue scattering coefficient using confocal microscopy," IEEE J. Sel. Top. Quantum Electron. **9,** 307–313 (2003).
33. W. F. Cheong, S. A. Prahl, and A. J. Welch, "A review of the optical properties of biological tissues," IEEE J. Quantum Electron. **26,** 2166–2185 (1990).
34. J. F. Beek, P. Blokland, P. Posthumus, M. Aalders, J. W. Pickering, H. J. C. M. Sterenborg, and M. J. C. van Gemert, "*In vitro* double-integrating-sphere optical properties of tissues between 630 and 1064 nm," Phys. Med. Biol. **42,** 2255–2261 (1997).
35. J. C. Finlay and T. H. Foster, "Effect of pigment packaging on diffuse reflectance spectroscopy of samples containing red blood cells," Opt. Lett. **29,** 965–967 (2004).
36. R. L. P. van Veen, W. Verkruysse, and H. J. C. M. Sterenborg, "Diffuse-reflectance spectroscopy from 500 to 1060 nm by correction for inhomogeneously distributed absorbers," Opt. Lett. **27,** 246–248 (2002).